Supporting Information

Intrinsic Chemical Reactivity of Solid-Electrolyte Interphase Components in Silicon-Lithium Alloy Anode Batteries Probed by FTIR Spectroscopy

*Ryan T. Pekarek,[1] Alec Affolter,[1,2] Lauryn L. Baranowski,[1] Jaclyn Coyle,[1,3,4,5] Tingzheng Hou,,[6,7] Eric Sivonxay[6], Brenda A. Smith,[5]Rebecca D. McAuliffe,[5] Kristin A. Persson,[6,7] Baris Key,[8] Christopher Apblett,[4] Gabriel M. Veith,[5] Nathan R. Neale[1]**

[1] Chemistry and Nanoscience Center, National Renewable Energy Laboratory, Golden, CO, 80401, USA
[2] University of Tennesee, Knoxville, Knoxville, TN 37996
[3] Department of Mechanical Engineering, University of Colorado Boulder, Boulder, Colorado 80309
[4] Sandia National Laboratories, Albuquerque, New Mexico 87123
[5] Oak Ridge National Laboratory, Oak Ridge, TN 37830
[6] Department of Materials Science and Engineering, UC Berkeley, Berkeley, CA 94720,
[7]Lawrence Berkeley National Lab, Berkeley, CA 94720
[8] Argonne National Laboratory, Lemont, IL 60439

*Corresponding author e-mail: nathan.neale@nrel.gov

Experimental

General. Toluene was dried and distilled from sodium benzophenone ketyl. Acetonitrile was dried and distilled over calcium hydride. Dibenzoyl peroxide (Alfa Aesar) was dried under vacuum (10^{-2} Torr) at room temperature for 24 h. Di-*tert*-butyl peroxide (Luperox DI, Sigma Aldrich) was degassed under vacuum (10^{-2} Torr) at room temperature. CAUTION!! Organic peroxides can be explosive when dry – only use small quantities (<1 g) and handle and store under inert gas atmosphere! Ethylene carbonate (EC, BASF), lithium hexafluorophosphate (BASF) and "Gen 2" electrolyte consisting of 1.2 M $LiPF_6$ solution in 70/30 (v/v) ethyl methyl carbonate (EMC)/EC (Tomiyama Fine Chemicals, Japan) were used as received. Nanoparticulate 'SiO_2' was purchased from NanoAmor (30–50 nm, Stock# 0141JS; Nanostructured & Amorphous Materials, Inc.), Fumed SiO_2 from Sigma-Alrich (0.2–0.3 μm, S5505), and Stöber SiO_2, and transferred into an Ar-filled glove box via antechamber at ambient temperature without thermal drying. All material handling and characterization was conducted in argon-filled glove boxes.

Silicon Nanocrystal (Si NC) Synthesis and Functionalization. Si NCs used for gassing studies were prepared using a custom-built RF plasma reactor, the details of which have been described elsewhere.[1] Briefly, 30 standard cubic centimeters per minute (sccm) of 10% silane (SiH_4) in helium along with 30 sccm argon carrier gas were passed through a capacitively-coupled plasma at a pressure of 3.00 Torr in a quartz reactor tube with 7 mm inner diameter and 9 mm outer diameter. A forward power of 75 W at 13.56 MHz was applied via an Advanced Energy Cesar 136 generator through an Advanced Energy VM1000 matching network (tuned to give a reflected power of 0–1 W) to a copper ring electrode. A grounded electrode was positioned downstream and separated by a 1.5 cm tall ceramic spacer. An Advanced Energy Z'Scan device was used to dynamically monitor the plasma conditions. Using the 1.5 cm spacing between the two electrodes as an estimate for the length of the plasma zone, the estimated residence time was 2.28 ms. Hydrogen-terminated Si NCs were collected downstream from the plasma on a 400-mesh stainless steel filter and transferred via load-lock to an inert-atmosphere glove box for collection. Based on

our prior work these as-prepared Si NCs exhibit diameters of 7.4 nm and are terminated by a mixture of surface hydrides (*SiH_x with x = 1−3).[2]

Si NCs used for FTIR studies were prepared similarly to that above using 7.1 sccm 100% SiH_4, 40 sccm Ar, and 140 sccm H_2 gas flows at 1.50 Torr in a 19 mm ID/25 mm OD quartz reactor tube at a forward plasma power of 250 W (0–1 W reflected power). These particles behave equivalently in functionalization chemistry reported in our prior work.[2] Their slightly smaller size (5.0 nm based on emission energy of functionalized samples) and higher proportion of silyl groups (*SiH_3) relative to 7.4 nm Si NCs (see DRIFTS data, main text) provided a greater signal-to-noise for the electrolyte chemical reactivity studies.

Si NCs were functionalized with benzoyl carboxylate and *tert*-butoxide ligands by combining as-synthesized Si NCs (6–10 mg) with dibenzoylperoxide (75 mg, 0.31 mmol) or di-*tert*-butylperoxide (40 mg, 0.27 mmol) and 1,1′-azobis(cyclohexanecarbonitrile) (ABCN, 10–15 mg, 0.04–0.06 mmol) radical initiator in toluene (~1.6 mL) heated to 100 °C for ~18 h. Following reaction, samples were diluted with toluene (2–5 mL) and sonicated for ~ 1 min followed by centrifugation at 12,000 × g for 10 min. The liquid was discarded and the solid material washed a 2nd time with toluene followed by centrifugation. Isolated solid particles were dried briefly under vacuum and characterized immediately by FTIR.

Lithium Silicate Synthesis. Lithium orthosilicate (Li_4SiO_4) powders were synthesized using the solid-state method[3, 4] governed by the reaction in equation 1:

$$2Li_2CO_3 + SiO_2 \rightarrow Li_4SiO_4 + 2CO_2 \quad [1]$$

SiO_2 (Alfa Aesar, Silicon(IV) Oxide, powder, 1.5um, 99.9%) and Li_2CO_3 (J.T. Baker, A.C.S. Reagent, Assay(Li_2CO_3)(by acidimetry) > 99%; product #2362-01) powders were mixed mechanically with a Li:Si molar ratio of 4:1 in an agate mortar. The mixtures obtained were calcined at 850°C for 5 hours then allowed to cool down to room temperature and mechanically milled again before a second heat treatment of 900°C for 8 hours. Ramp rates for heat treatments were set at 5°C/min.

Lithium metasilicate (Li_2SiO_3) powder (Aesar, discontinued stock) was calcined at 1000°C for 2 h to remove Li_2CO_3 contamination. Completed powders were stored in an inert atmosphere glovebox. Powder x-ray diffraction (XRD) was conducted on the lithium silicate powders using a Scintag X1 X-ray diffractometer with a Cu-K_α x-ray source operating at 45kV and 40 mA to confirm composition.

Electrolyte Reactions. As-prepared *SiH_x-Si NCs, benzoyl carboxylate-Si NCs ($PhCO_2$–Si), *tert*-butoxide-Si NCs (tBuO–Si), 30–50 nm NanoAmor Si, Stöber SiO_2, S5505 Fumed SiO_2, Li_2SiO_3, and Li_4SiO_4 (~25 mg each) were combined with electrolyte (~0.75 g each) and allowed to soak for 1–3 days. After this time, particles were diluted with acetonitrile (2–5 mL) followed by an equal volume of toluene and then centrifuged at 12,000 × g for 10 min except for the lithium silicate samples, which required ~20 min centrifugation to fully separate from the liquid. The liquid was discarded, and the solid material washed a 2nd time with acetonitrile/toluene followed by centrifugation. Isolated solid particles were dried briefly under vacuum and characterized immediately by FTIR.

Supporting Information

Fourier Transform Infrared Spectroscopy. Diffuse Reflectance Infrared Fourier Transform Spectroscopy (DRIFTS) measurements on materials before and after electrolyte reactions were performed on a Bruker Alpha FTIR spectrometer inside an Ar-atmosphere glovebox by depositing powder as a toluene slurry onto gold-coated Si wafers and drying at 60 °C. Spectra for 1.2 M $LiPF_6$ in EC and Gen 2 electrolytes, di-*tert*-butyl peroxide, dibenzoyl peroxide were collected using the same instrument with an attenuated total reflectance (ATR) attachment. All spectra were collected by averaging 24 scans at 2 cm^{-1} resolution and were processed using baseline correction.

Classical molecular dynamics (MD): MD simulations were performed using the Large Scale Atomic/Molecular Massively Parallel Simulator (LAMMPS)[5] code for electrolytes of 1.2 M $LiPF_6$ in EC or Gen2 electrolyte (1.2 M $LiPF_6$ in 3:7 (w/w) EC/EMC). To characterize the intra- and inter-molecular interactions, non-polarizable force fields were employed. The bonded interactions (bonds, angles, dihedrals, and impropers) were modeled as harmonic functions and the nonbonded included van der Waals interactions and Coulombic forces. The bonded and non-bonded parameters for EC and EMC were obtained from the Optimized Potentials for Liquid Simulations All Atom (OPLS-AA) force fields,[6, 7] the PF_6^- anion from Lopes et al.,[8] and the lithium cations from Jensen et al.[9] The MD simulation unit contained 1,500 solvent molecules and between 126-166 salt molecules were used to achieve different concentrations. The systems were equilibrated for 2ns in the isothermal-isobaric ensemble (constant NPT) using the Parrinello–Rahman barostat to maintain a pressure of 1 bar and a temperature of 298 K with a time constant of 1ps. An annealing process was conducted to further guarantee that all systems were melted and to avoid local configuration confinement. This process entailed heating from 298 K to 400 K for 1ns, and maintained at 400 K for 1 ns, and subsequently annealed from 400 to 298 K in 1 ns. Finally, the production runs of 10 ns were conducted in the canonical ensemble (NVT) under Nose-Hoover thermostats with a time constant of 1 ps at 298 K.

Simulated FTIR spectra The simulated FTIR spectra of surface adsorbed EC molecules were obtained using Density Functional Perturbation Theory (DFPT) as implemented in the Vienna Ab-initio Simulation Package (VASP).[10, 11] The (111) Si slab consisted of 4 Si layers, obtained from a 4 x 4 x 4 supercell of FCC Si, with an added 10Å of vacuum. The slab was generated using the python materials genomics software package (pymatgen),[12] and all atomic positions were optimized using VASP. EC was then added above the slab with the C=O bond perpendicular to the slab surface. With the bottom 3 layers of Si fixed, the structure was again optimized. Vibrational eigenmodes and frequencies were computed using DFPT with all atoms fixed, except for the EC atoms and the coordinated Si. Relative intensities were computed from the Born Effective Charge tensor.[13] All first-principles calculations utilized the Perdew-Burke-Ernzerhof formulation[14] of the generalized gradient approximation functional with projector-augmented wave potentials[15] with a plane-wave kinetic-energy cutoff of 520eV and a k-point mesh of 2 x 2 x 1.

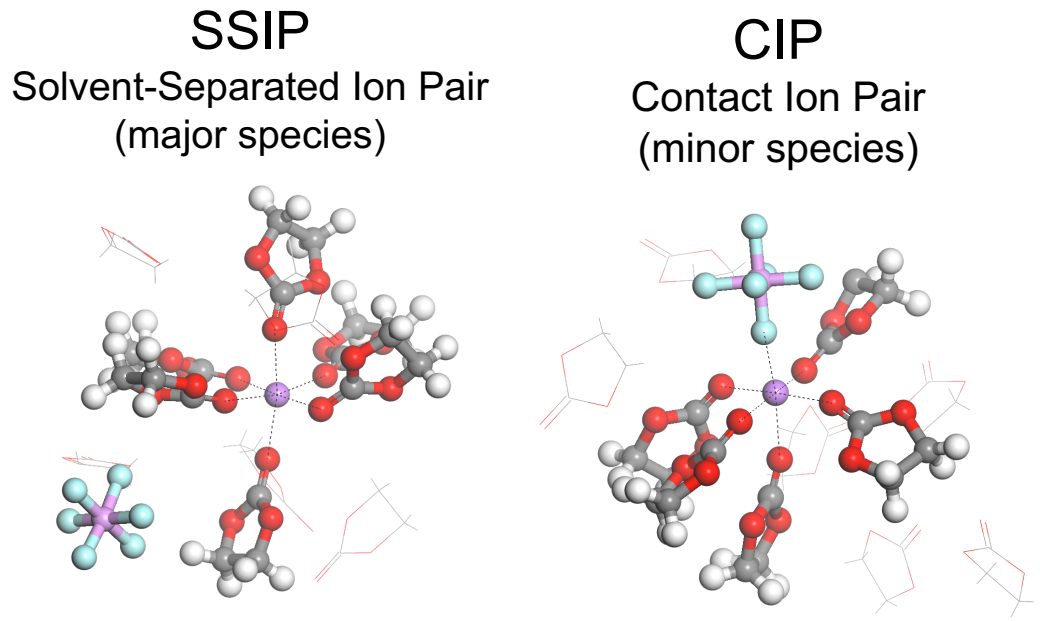

Figure S1. Molecular structures of a solvent-separated ion pairs (SSIP) $[Li^{+}(EC)_{6-x}(EMC)_{x}]PF_6^{-}$ as well as the contact ion pair (CIP) $[Li^{+}(EC)_{5-x}(EMC)_{x}PF_6^{-}]$. Shown are coordination by EC only, but EMC also competes for Li-ion coordination in the Gen2 electrolyte.

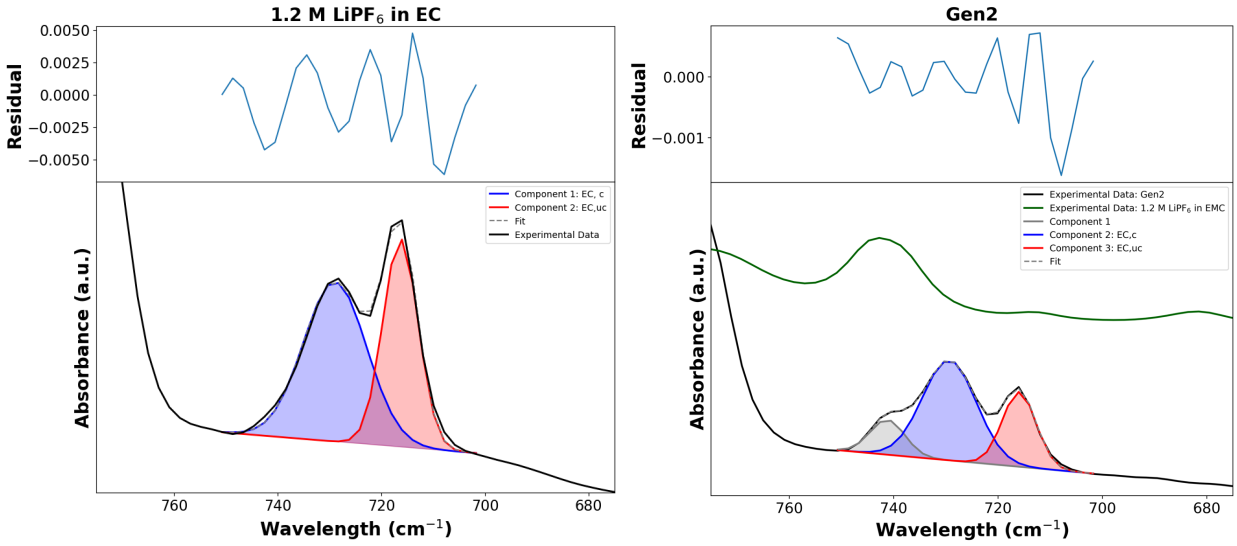

Figure S2. Integrated areas of FTIR peaks from $\delta_{C=O}$ EC ring bending modes for c EC (728 cm^{-1}, blue) and uc EC (716 cm^{-1}, red) in 1.2 M $LiPF_6$ in EC (Left) and Gen2 (Right) electrolytes. The 3rd peak (grey) in the figure at Right is a vibrational mode associated with EMC (as shown by the green trace: 1.2 M $LiPF_6$ in EMC).

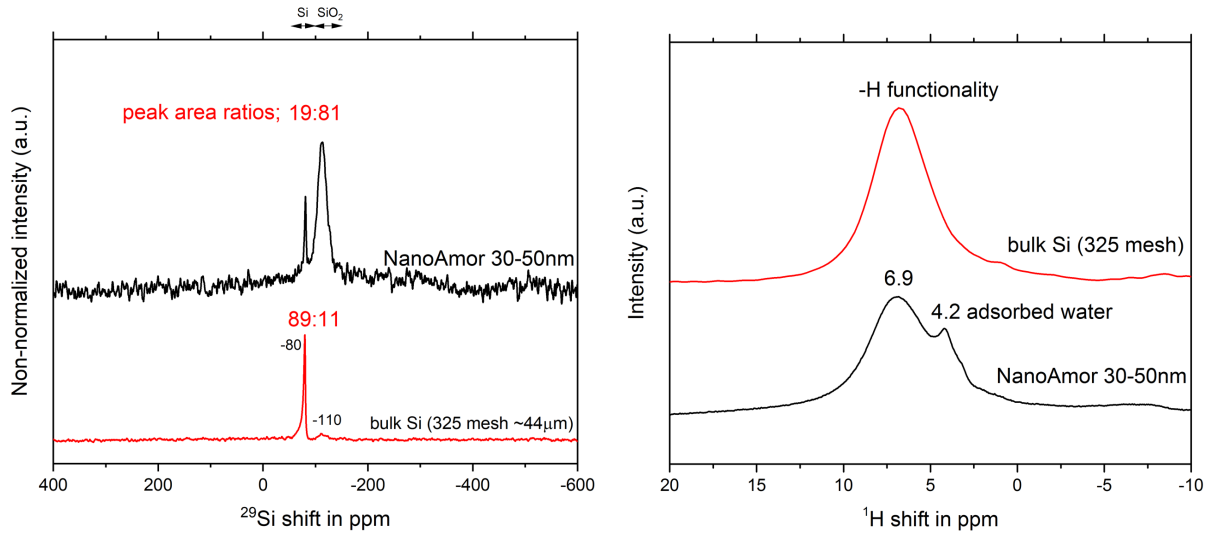

Figure S3. ^{29}Si (Left) and ^{1}H (Right) solid-state nuclear magnetic resonance (NMR) spectra of commercially supplied NanoAmor 30–50 nm Silicon as well as 325 mesh bulk Si supplied by Sigma Aldrich.

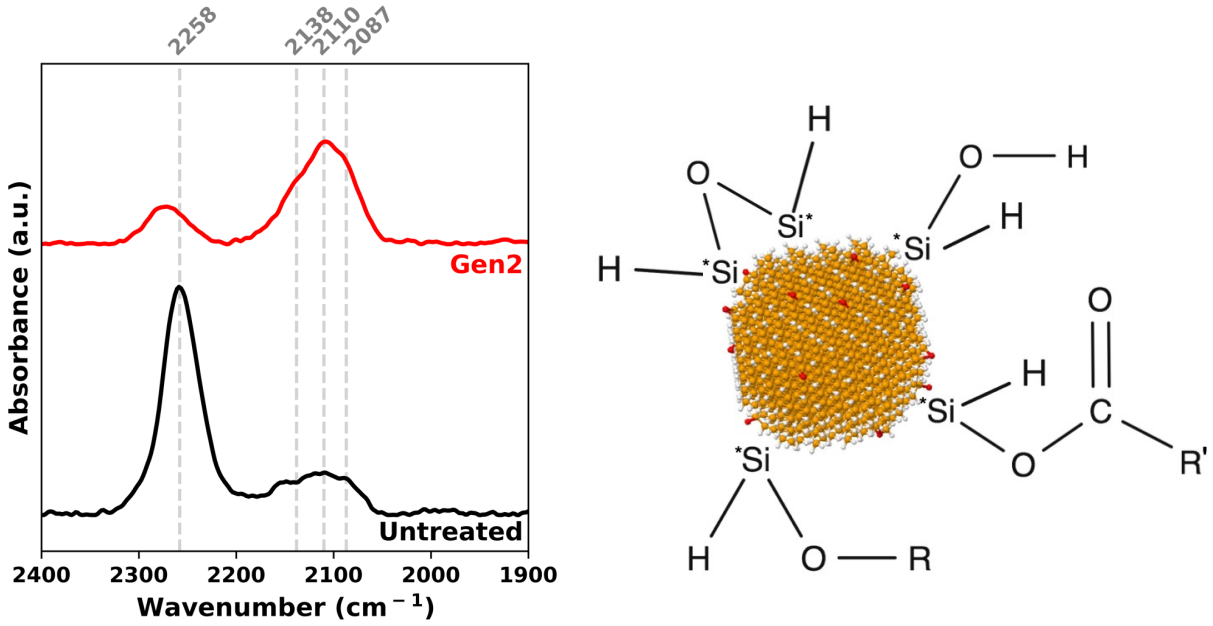

Figure S4. Left: FTIR spectra of ν_{Si-H} region for 30–50 nm NanoAmor Silicon before (black) and after (red) exposure to Gen2 electrolyte. Following reaction, an increase in intensity of clean *SiH_x (2087–2138 cm^{-1}) relative to oxidized (O_y)*SiH_x (2258 cm^{-1}) is apparent, suggesting the electrolyte exposure induces dissolution of SiO_2. Right: Chemical schematic of oxygen-containing species at the surface resulting in the back-bonded (O_y)*SiH_x stretch derived from a number of chemical functionalities such as *Si–O*Si, *Si–OH, *Si–OR, *Si–OC(O)R', etc.

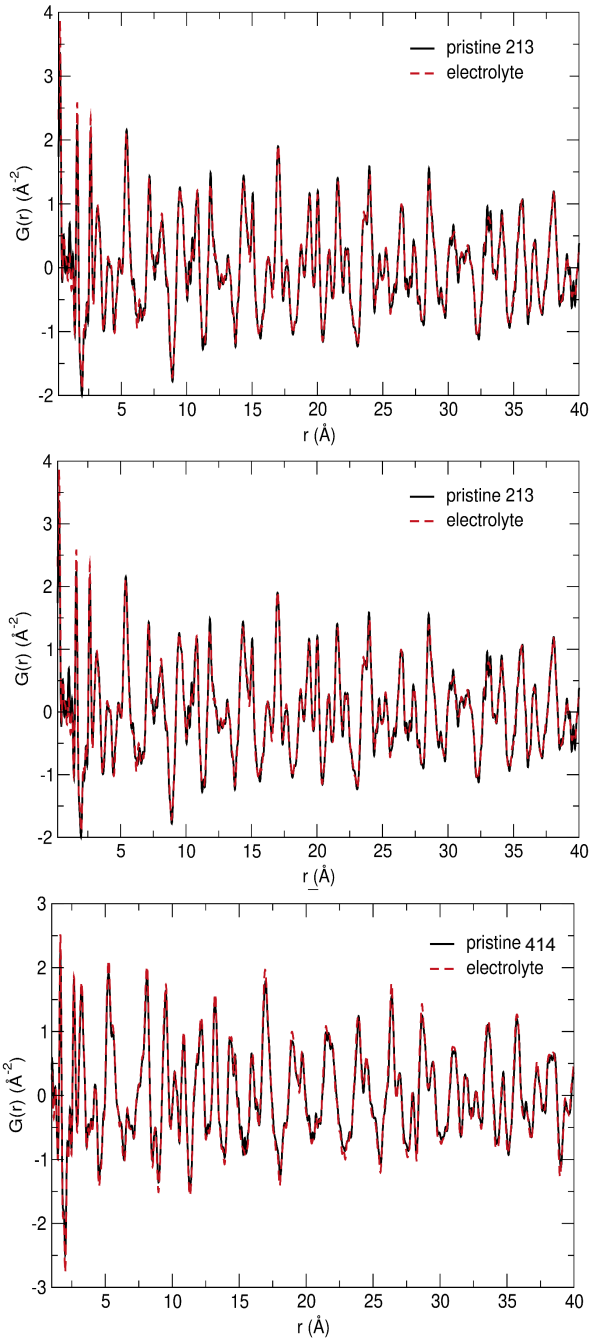

Figure S5. Neutron pair distribution function (PDF) data collected for Li_2SiO_3 (top; "pristine 213"), $Li_2Si_2O_5$ (middle; "pristine 225"), and Li_4SiO_4 (bottom; "pristine 414") for the raw material (black line) and material following exposure to electrolyte (red dashed line). The samples were analyzed on the Nanoscaled-Ordered Materials Diffractometer (NOMAD) located at the Spallation Neutron Source. This instrument is ideally configured to collect data suitable for PDF analysis which is useful for identifying structural correlations within amorphous material. Furthermore, neutrons are especially sensitive to low *Z* elements like Li and O, allowing for structural determination of materials containing these elements.

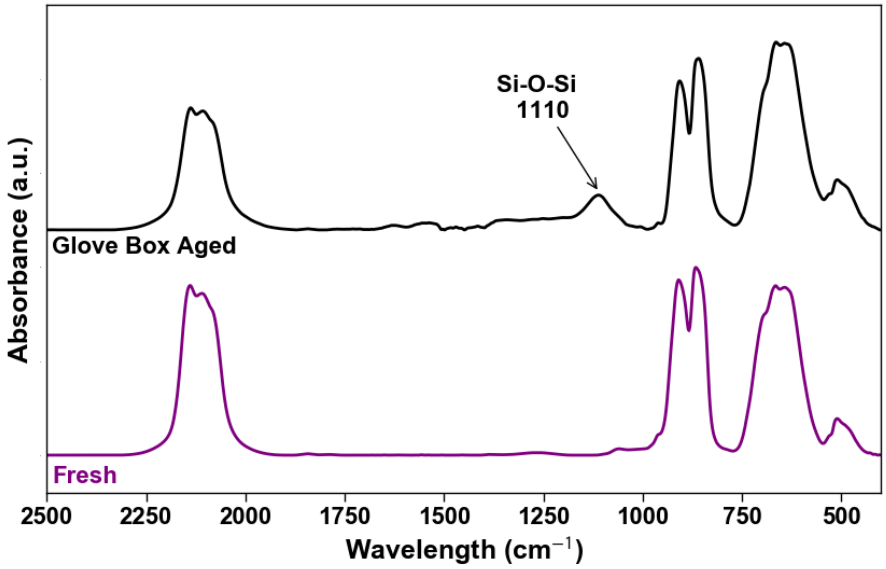

Figure S6. FTIR spectra of as-grown Si NCs from nonthermal plasma synthesis before (purple) and after (black) storage in an argon-filled glove box for 2 weeks. A large increase in intensity, slight shift to higher energy, and broadening of the $\nu_{Si-O-Si}$ stretch near 1100 cm^{-1} is evident in the stored sample resulting from oxidation. This experiment shows that even under rigorous conditions (<0.5 ppm H_2O and <0.1 ppm O_2 atmosphere), preventing surface oxidation from these highly oxophilic, hydride-terminated silicon nanoparticles is extremely challenging.

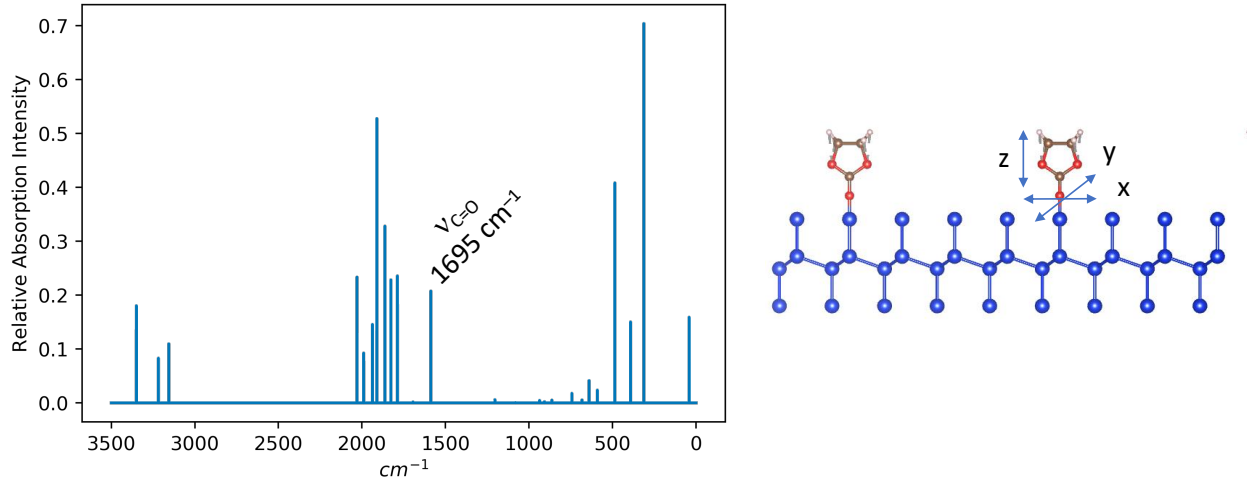

Figure S7. FTIR simulations from DFPT calculations of EC coordinated to a surface *Si showing the strong, intense absorption at 1695 cm^{-1}.

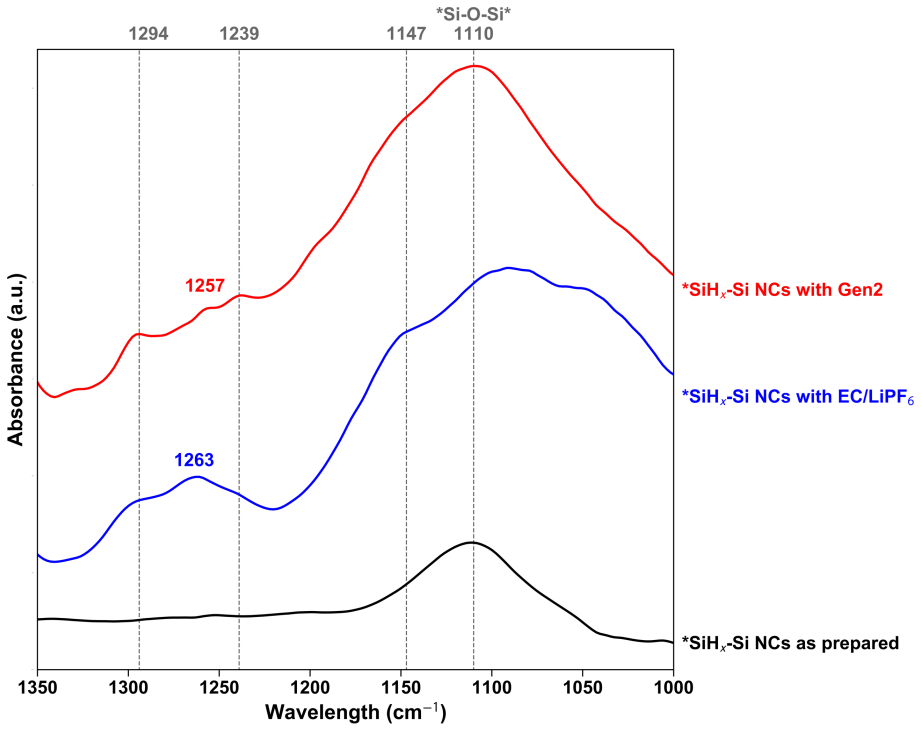

Figure S8. FTIR spectra from 1000–1350 cm^{-1} for the solid product remaining following reaction between *SiH_x-terminated Si NPs and Gen2 or 1.2 M $LiPF_6$ in EC electrolytes.

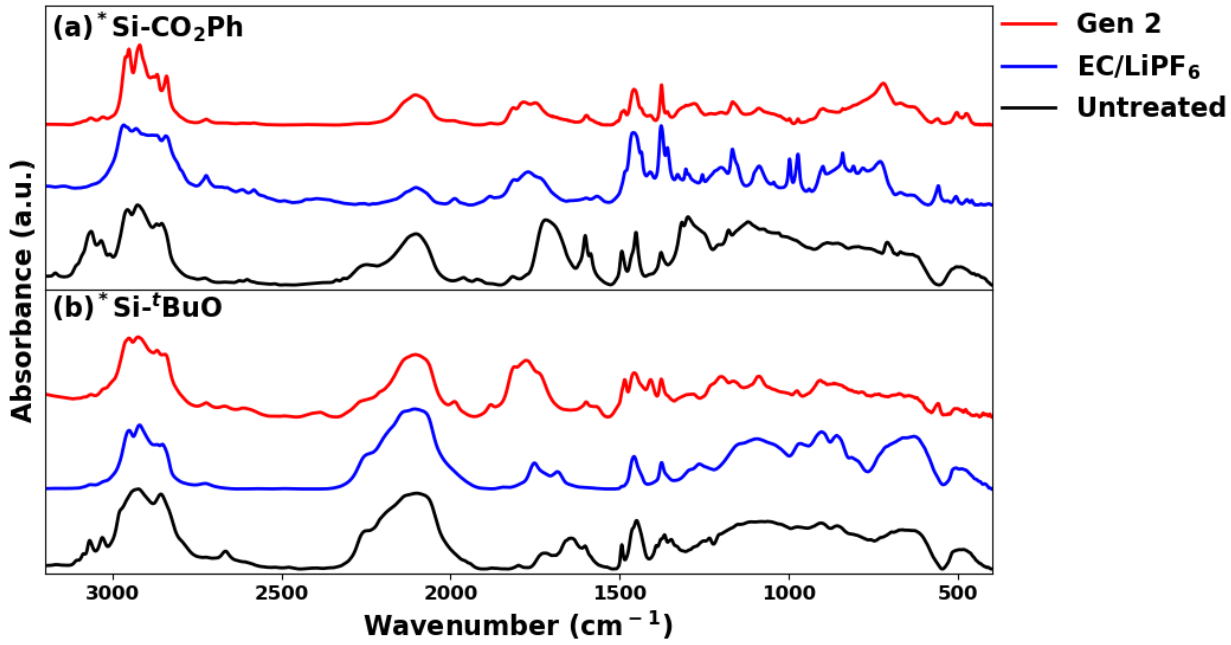

Figure S9. FTIR spectra from for the solid product remaining following reaction between (a) silyl ester PhC(O)O-Si or (b) silyl ether ^{t}BuO-Si NCs and Gen2 (red) or 1.2 M $LiPF_6$ in EC (blue) electrolytes. FTIR spectra for as-prepared silyl ester PhC(O)O-Si and silyl ether ^{t}BuO-Si NCs prior to reaction with electrolytes are shown in black.

References

1. L. Mangolini, E. Thimsen and U. Kortshagen, *Nano Lett.*, 2005, **5**, 655-659.
2. L. M. Wheeler, N. C. Anderson, P. K. B. Palomaki, J. L. Blackburn, J. C. Johnson and N. R. Neale, *Chem. Mater.*, 2015, **27**, 6869-6878.
3. E. Carella and M. T. Hernandez, *Ceram. Int.*, 2014, **40**, 9499-9508.
4. H. Pfeiffer, P. Bosch and S. Bulbulian, *J. Nucl. Mater.*, 1998, **257**, 309-317.
5. S. Plimpton, *J Comput Phys*, 1995, **117**, 1-19.
6. W. L. Jorgensen, D. S. Maxwell and J. Tirado-Rives, *J. Am. Chem. Soc.*, 1996, **118**, 11225-11236.
7. G. A. Kaminski, R. A. Friesner, J. Tirado-Rives and W. L. Jorgensen, *J. Phys. Chem. B*, 2001, **105**, 6474-6487.
8. J. N. Canongia Lopes and A. A. H. Pádua, *J. Phys. Chem. B*, 2004, **108**, 16893-16898.
9. K. P. Jensen and W. L. Jorgensen, *J. Chem. Theory Comput.*, 2006, **2**, 1499-1509.
10. G. Kresse and J. Furthmüller, *Computational Materials Science*, 1996, **6**, 15-50.
11. G. Kresse and J. Furthmüller, *Phys. Rev. B*, 1996, **54**, 11169-11186.
12. S. P. Ong, W. D. Richards, A. Jain, G. Hautier, M. Kocher, S. Cholia, D. Gunter, V. L. Chevrier, K. A. Persson and G. Ceder, *Computational Materials Science*, 2013, **68**, 314-319.
13. D. Karhánek, T. Bučko and J. Hafner, *Journal of Physics: Condensed Matter*, 2010, **22**, 265005.
14. J. P. Perdew, K. Burke and M. Ernzerhof, *Phys. Rev. Lett.*, 1996, **77**, 3865-3868.
15. P. E. Blöchl, *Phys. Rev. B*, 1994, **50**, 17953-17979.